Progress In Electromagnetics Research M, Vol. 84, 85–93, 2019

Laser Systems for Distant Monitoring of Nanopowder Combustion

Lin Li, Petr A. Antipov, Andrei V. Mostovshchikov, Alexander P. Ilyin, and Fedor A. Gubarev*

Abstract—The paper discusses the application of laser illumination and brightness amplification techniques for studying the process of high-temperature combustion of aluminum and iron nanopowders and their mixtures. The laser equipment for visualization based on solid-state laser illuminator, brightness amplifier on copper bromide vapors and high-speed camera is considered. These approaches allow the increase of monitoring distance to 50 cm, which is important for high-temperature processes imaging. The video images allow studying the surface morphology changes during high-temperature combustion identifying the main stages of combustion, spreading of the heat waves and cooling.

1. INTRODUCTION

Nowadays the keen interest of scientists is concentrated in the nanoparticle industry, connected with materials combustion [1]. Particularly, aluminum-based materials obtained by high-temperature combustion of nanopowders in air offer a number of interesting and potentially high impact commercial opportunities [1–9]. Combustion of aluminum and iron nanopowders and their mixtures proceeds at temperatures above 2000°C and is accompanied by a bright gloving and the scattering of combustion products in some cases [10, 11]. Moreover, the combustion of nanopowders is a fast process with a flow rate of a few millimeters or centimeters per second. These factors make it difficult to study combustion using visual methods.

Opportunities for observing high-temperature high-speed processes, in particular, nanopowder combustion processes, appear with the use of laser radiation and high-speed video recording [10–17]. When an observation object is illuminated by narrow-band laser radiation, a part of the radiation is reflected from the surface. If the intensity of the reflected radiation is higher than the intensity of the flame, it can be filtered and recorded by the camera [11]. If the intensity of the reflected radiation is comparable to the radiation of the flame, it should be amplified in brightness, and then recorded.

Gaseous metal vapor active media have unique characteristics such as narrow natural bandwidth of amplification, high single pass gain, high pulse repetition frequency, operation in the visible spectral region, high average power and ability to control laser radiation parameters [18–26], which make them appropriate for use as brightness amplifiers in laser monitors. These imaging systems allow observation through the flame or plasma and visualization of the processes shielded by intensive background lighting. In particular, they can be used to perform diagnosis of the substance surface burning with high intensity of light emission during the combustion or plasma induced processes [10–12, 27–30]. For the first time, an active optical system with brightness amplification was used to study the aluminum nanopowder combustion in [12].

In this work, we discuss the application of laser illumination and brightness amplification for studying the process of high-temperature combustion of aluminum nanopowder and its mixture with iron nanopowder. In particular, the laser equipment for visualization based on solid-state laser illuminator,

Received 1 June 2019, Accepted 10 August 2019, Scheduled 25 August 2019
* Corresponding author: Fedor Alexandrovich Gubarev (gubarevfa@tpu.ru).
The authors are with the National Research Tomsk Polytechnic University, Russia.

brightness amplifier on copper bromide vapors and high-speed camera is considered, and the results of combustion visualization are presented.

2. EXPERIMENTAL DETAILS

During the experiments, the nanopowder in the form of the sample of rectangular elongated shape was placed on a 4 mm thick aluminum substrate. The sample weight was more than 3 g to provide the combustion duration enough for visual diagnostics. The samples had approximately the same dimensions $20 \times 5 \times 3\,\text{mm}^3$ ($0.3\,\text{cm}^3$ volume) and were prepared manually using the mold. Therefore, the density of the sample was $\sim 10\,\text{g/cm}^3$. We studied the combustion of pure nanoAl powder and nanoAl+nanoFe mixture in the percentage volume proportion of 60/40. The particle size distribution of the powders was close to the logarithmic normal with the maximum of 80 nm for Al nanopowder and 110 nm for Fe nanopowder. Fig. 1 presents the photomicrographs of the initial nanoAl and nanoFe particles obtained using a scanning transmission electron microscope Jeol 2100. Fig. 2 shows the typical view of the initial samples and combustion products. We can see that nanoAl+nanoFe powder has a distinct dark color compared to nanoAl powder. Moreover, the presence of iron gives a yellow color to the combustion products.

The temperature during the combustion of aluminum-based mixtures can reach 2500°C and cause the intensive broadband light emission according to the Wien's displacement law. This intensive background lighting interferes the visual monitoring. Figs. 3 and 4 present the frames of video recording

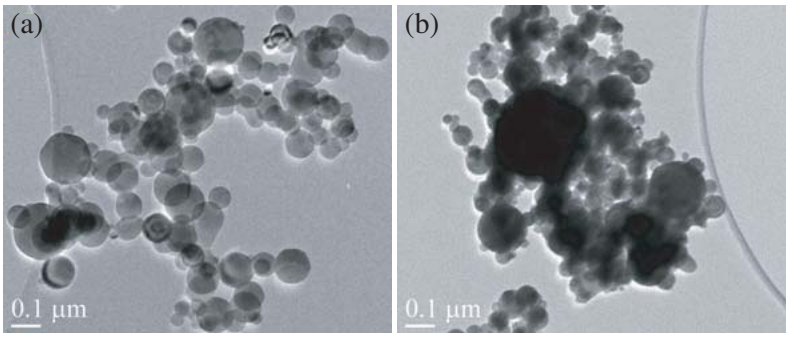

Figure 1. STEM photomicrographs of the initial (a) nanoAl and (b) nanoFe powders.

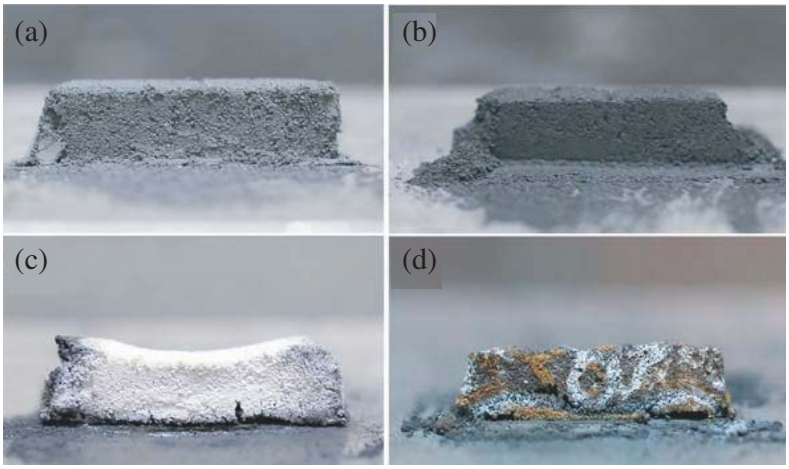

Figure 2. The typical view of the initial samples of (a) nanoAl and (b) nanoAl+nanoFe, and the combustion products of (c) nanoAl and (d) nanoAl+nanoFe.

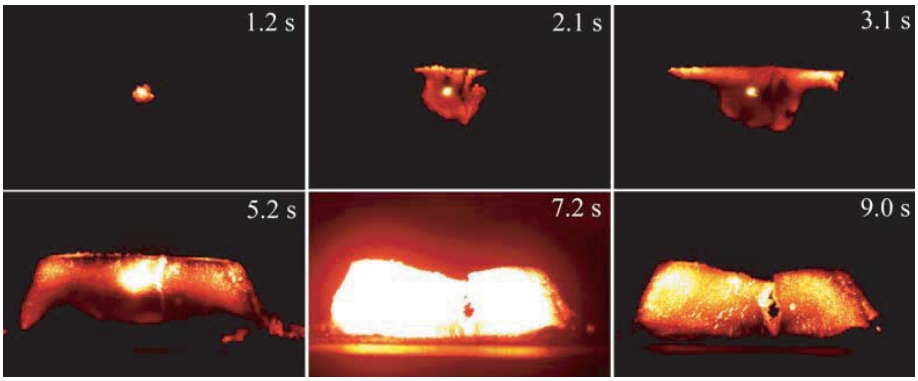

Figure 3. Frames of the nanoAl combustion imaging in its own light at different moments of time, relative to the moment of ignition start.

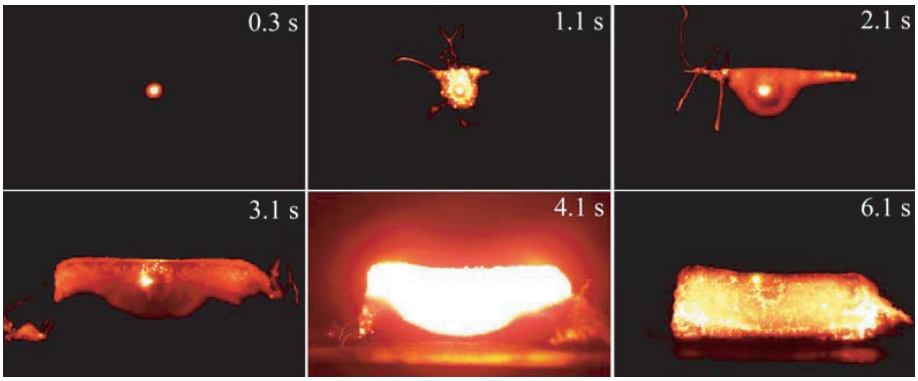

Figure 4. Frames of the nanoAl+nanoFe mixture combustion imaging in its own light at different moments of time, relative to the moment of ignition start.

of nanoAl and nanoAl+nanoFe combustion in its own light. We see that the combustion ignition and burning of nanoAl run smoothly and evenly (Fig. 3). Combustion of nanoAl+nanoFe mixture runs almost similar to the combustion of nanoAl with the exception of the initial stage. There is a thermal explosion at the beginning (Fig. 4). The recording of the combustion in its own light (without laser monitor or laser illumination) was realized by means of USB digital camera ELP-USBFHD01M-MFV. To prevent the camera saturation, a low-pass filter was installed.

Direct recording of combustion in its own light allows to judge the process generally but does not allow to study the surface of the sample, especially during the second high-temperature stage. In order to visualize the surface of the sample, it is necessary to provide that the light reflected from the object surface be much more intense than the light emitted by the flame of the burning sample. The flame emits intense radiation in a wide spectral region, while the spectral brightness of the flame is orders of magnitude less than the spectral brightness of the laser. Therefore, to visualize the surface of the burning sample, we propose to use laser illumination and laser monitoring. The surface of the aluminum nanopowder has a reflection of $\sim 10\%$, the reflection of the surface of the nanoAl+nanoFe mixture is $\sim 2\%$. Thus, when using laser illumination, it is necessary to ensure bright enough for the camera to register the image on the one hand, and to exclude the influence of the illumination radiation on the ignition and combustion on the other hand. Unlike laser illumination, a laser monitor is a projection microscopic system that gives magnification allowing micro details visualization. In addition, this system amplifies the brightness of the image, allowing recording significantly lower reflected radiation.

The first laser techniques used in our work was using a compact laser monitor built based on the laboratory-made copper bromide brightness amplifier. Fig. 5 shows the scheme of the laser monitor.

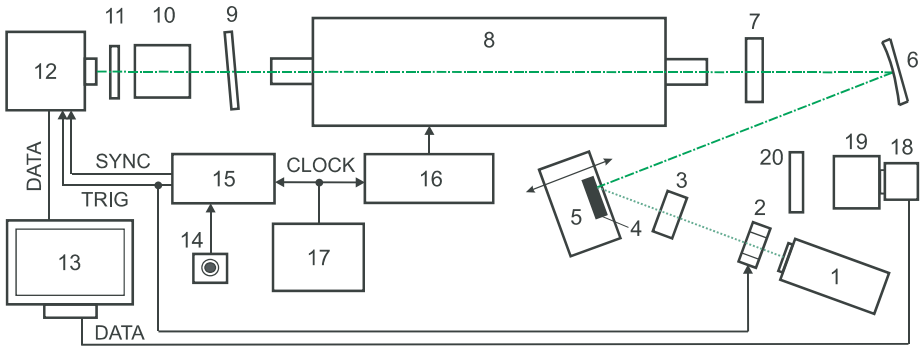

Figure 5. Scheme of the laser monitor. 1 — igniting laser, 2 — mechanical shutter, 3 — lens, 4 — object, 5 — stage, 6 — concave mirror, 7 — lens, 8 — brightness amplifier, 9 — gray filter, 10 — objective, 11 — band-pass filter, 12 — high-speed camera, 13 — PC, 14 — start button, 15 — control unit, 16 — pumping circuit, 17 — pulse generator, 18 — USB-camera, 19 — objective, 20 — band-pass filter.

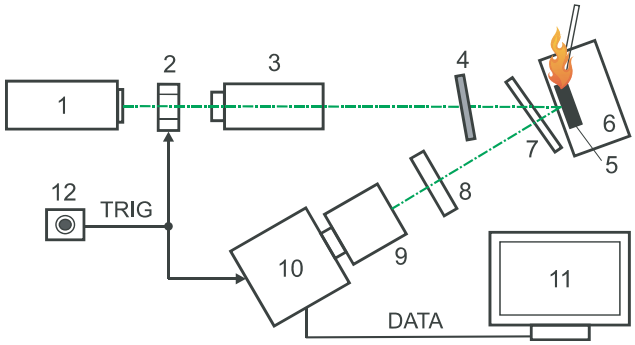

Figure 6. Scheme of imaging using laser illumination. 1 — illuminating laser, 2 — mechanical shutter, 3 — beam expander, 4 — diffuser, 5 — object, 6 — stage, 7 — protecting glass plate, 8 — band-pass filter, 9 — objective, 10 — high-speed camera, 11 — PC, 12 — start button.

The gas-discharge tube of the brightness amplifier had the aperture of 1.5 cm and the length of the active area of 50 cm. The tube generated 20-μJ pulse amplified spontaneous emission (ASE) at 510.6 and 578.2 nm wavelengths operating at 20 kHz pulse repetition frequency. The image of the object *5* in this scheme was formed by a concave mirror *6* and lens *7* (Fig. 5). It was amplified by the brightness amplifier *8* and recorded by a high-speed camera *12*. We used monochrome camera Photron Fastcam SA1, which was operated in external sync mode to provide synchronization with the pulses of ASE. Camera triggering was provided simultaneously with opening of the mechanical shutter. Objective *10* with filters *9* and *11* served for image scaling and attenuation. The mirror-based scheme of laser monitor was suggested in [31], we proposed a scheme of a laser monitor in which the image was formed by a mirror and an objective carried out the coupling with a high-speed camera. To focus the radiation on the object of study, we used a mirror with a radius of curvature of 3 m. The use of a 1-meter focal length lens *7* made it possible to collimate the beam of ASE, reducing the focal length of the projection system up to 0.5 meters and diameter of the observation area up to ~ 4 mm. The nanopowder sample was placed on the stage equipped with a linear translator to adjust the focus of the system. The observation area of the laser monitor envelops the place of laser ignition.

The ignition of the combustion process was provided by 532 nm continues wave radiation of DPSS laser. According to [32], ablation and ignition should occur at a certain threshold fluence. The threshold value for 532 nm radiation was 50 MBT of continuous wave radiation focused on the sample by 9.5 cm focus lens. Therefore, the ignition was conducted by the average output power 200 mW focused on the sample to provide the certain combustion ignition. It was enough to provide the certain combustion ignition from one side, and did not lead to ablation from the other side.

The second scheme of high-speed imaging used in this work was the scheme with laser illumination. We used the scheme with laser illumination early with 532 nm wavelength and 5 mW power continuous DPSS laser in [11]. It was shown that the method of visualization with external laser illumination is good for panoramic view of the processes. It allowed estimating roughly stages and velocity of processes, and characterizing the behavior of the sample combustion. The drawback of the technique used in [11] was a speckle structure of images. The size of speckles reached ~ 0.2 mm and did not resolve the detailed study of the sample surface. In the present work, we increased the illumination power to 50 mW and installed x10 beam expander to provide the uniform illumination of the sample surface. Fig. 6 shows the scheme of imaging with laser illumination. An open fire from a match ignited the combustion. The 532 nm band-pass filter with 10 nm bandwidth was used to block the wideband background lighting of the flame. We used the same monochrome camera in these experiments, which was operated in internal sync mode.

3. RESULTS

The frames of the high-speed imaging of the combustion process of nanoAl and nanoAl+nanoFe powder mixtures using the laser monitor are shown in Figs. 7 and 8. In Figs. 9 and 10 we present the frames

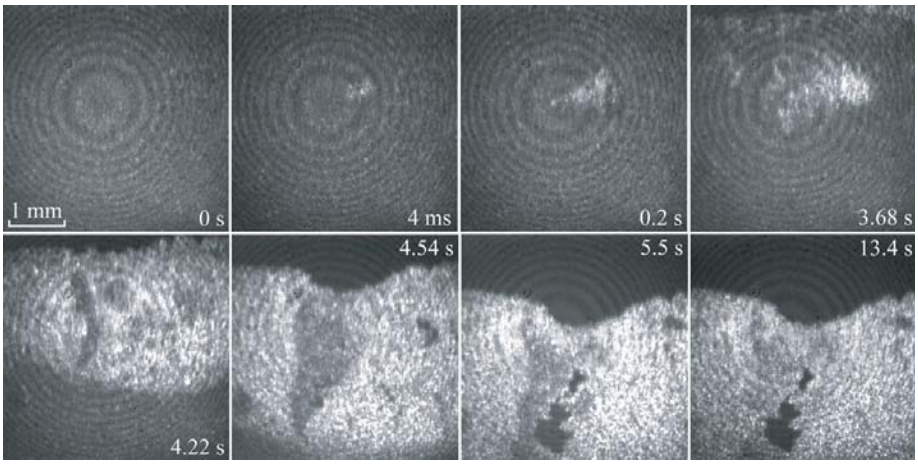

Figure 7. Frames of the nanoAl combustion imaging obtained by the laser monitor at different moments of time from the ignition start.

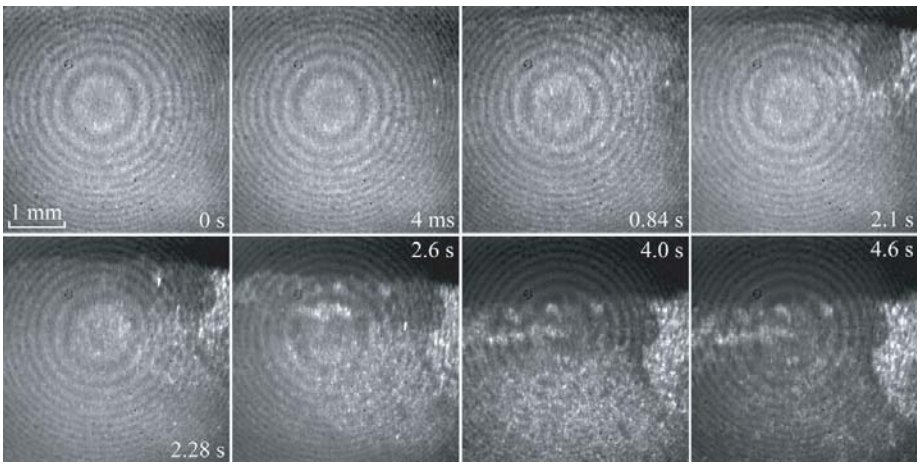

Figure 8. Frames of the nanoAl+nanoFe mixture combustion imaging obtained by the laser monitor at different moments of time from the ignition start.

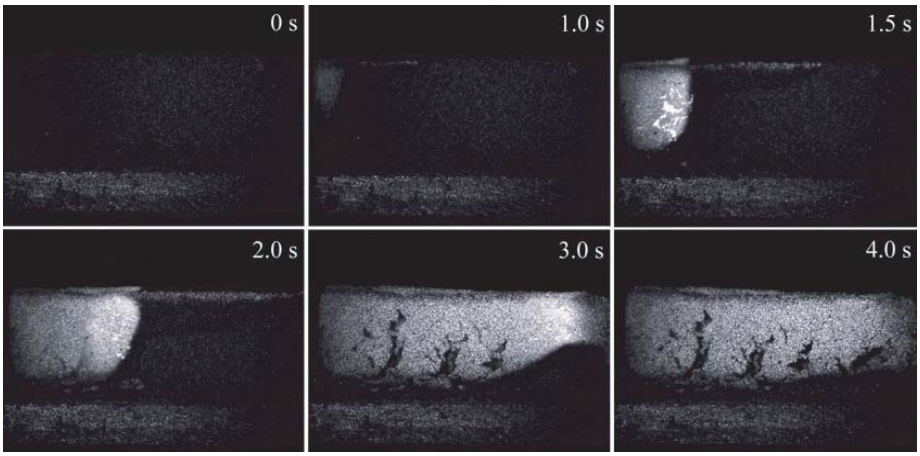

Figure 9. Frames of the high-speed imaging of nanoAl combustion obtained with laser illumination at different moments of time from the ignition start.

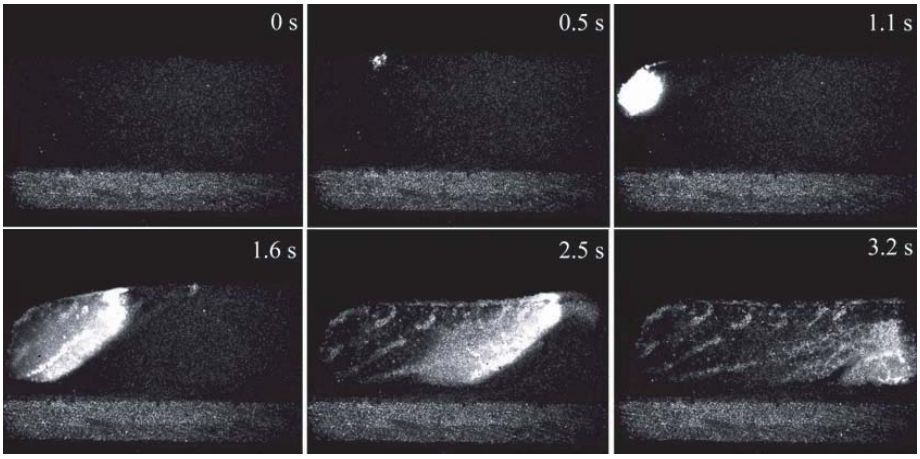

Figure 10. Frames of the high-speed imaging of nanoAl+nanoFe combustion obtained with laser illumination at different moments of time from the ignition start.

of the high-speed imaging of the combustion process of the same powders using laser illumination. In comparison with [10, 11], the area of observation of laser monitor in the present work is larger. It allows monitoring the agglomerate formation; however, it is not well suited for low-temperature stage control. Because of the additional optical element present in the scheme, we have Newton's rings disturbing the observation of the first combustion stage which accompanied by slight surface changing only. The advantage of this scheme is revealed in study of the second high-temperature combustion stage. Brightness amplification fully suppresses the intensive background lighting emitted by the burning sample allowing the control of the surface reflection. As a result, even small changes like deepening, dimples, or bulges are possible to be detected. The laser monitor scheme can be designed with the proper magnification, required for the particular task. In [10], the agglomerates with the size of 5–30 μm were observed with Navitar DO-5095 objective lens. The laser monitor in the present work resolved the agglomerates observation with the size more than 25 μm.

External laser illumination in combination with narrow-band filtering also makes it possible to suppress the intense background lighting of the burning sample. However, it is extremely difficult to see the first wave of combustion of aluminum nanopowder or its mixture with iron nanopowder. This is because the filter is chosen so as not to light the camera matrix up during the entire combustion

process. In fact, the filter is chosen for the brightness of the second high-temperature wave of combustion. In addition, on the first combustion stage, the reflection coefficient and surface morphology of aluminum nanopowder changes only slightly [10], and it is difficult to distinguish these changes without brightness amplification. The advantage of the laser illumination method is the possibility of panoramic observation of the entire sample, which is important for getting general information about the nature of combustion. The aluminum nanopowder burns evenly to form the smooth structure of white color (ideally). Combustion of the mixture of nanoAl+nanoFe spreads in separate bands, resulting in a yellowish structure with white stripes. In this case, the ignition method significantly affects the appearance of the sample and the behavior of combustion. When using laser ignition in the central part of the sample, a ring of aluminum-containing products is formed at the ignition site (Fig. 2(d)). When being ignited by open fire at the edge, the product structure is striped. The white stripes are products of combustion of aluminum nanopowder; yellow ones are products of the combustion of iron nanopowder.

In contrast to the laser projection system with brightness amplification, the laser illumination method does not provide complete suppression of background lighting, which makes it possible to estimate visually the surface temperature. Observing the burning of aluminum nanopowder in this way, the bright glow in the cracks is noted, which indicates a higher temperature inside them (Fig. 8). The front of the second wave of combustion also has a higher temperature. Observing the combustion of nanoAl+nanoFe mixture, the bright luminescence at the moments of flashes at the beginning of the first wave of combustion (0.5 second in Fig. 9), in the cracks and at the combustion front, draws attention.

4. CONCLUSION

The results of monitoring the high-temperature combustion of nanoAl and nanoAl+nanoFe powders are presented. Observing with laser illumination, we can monitor the whole sample and observe structural surface changes. During combustion of aluminum nanopowder, we can estimate the propagation velocity of the first and second combustion waves, the shape of the combustion front in different parts of the sample, the appearance and propagation of cracks associated with the formation of agglomerates of combustion products and the shrinkage of the surface. During the combustion of a mixture of nanoAl+nanoFe, combustion heterogeneity is clearly observed, leading to the formation of strips with different structures on the sample surface. The shape of the combustion front for the nanoAl+nanoFe mixture differs from the shape of the combustion front of nanoAl. The catalytic effect of the addition of iron nanopowder and the combustion rate of aluminum nanopowder when adding iron nanopowder increased from 8.6 to 10.6 mm/sec should also be noted.

The video images obtained with a copper bromide laser monitor allow monitoring the main stages of the combustion process including starting of combustion, spreading of the heat waves and cooling. The laser monitor combines a microscopic scheme, an illuminator, and a narrow-band brightness amplifier. Due to this, laser monitors allow investigation of the object surface despite the intensive background lighting. This allows more detailed observation of the agglomeration of products during combustion, the appearance of cracks and discontinuities. When combining the observation area with the laser ignition area, the laser monitor allows observing the ignition process. The laser monitor is a narrow-band system, so the igniting laser radiation does not affect the images of the laser monitor, no matter how bright the igniting radiation is.

Application of a mirror-based scheme has the advantage of observing the surface of burning materials at a considerable distance from the optical elements (50 cm in this work). It makes this system suit for observing the combustion of thermite mixtures and others accompanied by the scattering of products. For the complex analysis of the combustion processes, it is suggested to use both techniques.

ACKNOWLEDGMENT

The research was carried out at Tomsk Polytechnic University within the framework of Tomsk Polytechnic University Competitiveness Enhancement Program and supported by The Ministry of Science and Higher Education of the Russian Federation, Project No. 11.1928.2017/4.6.

REFERENCES

1. Zarko, V. E. and A. A. Gromov, *Energetic Nanomaterials: Synthesis, Characterization, and Application*, Elsevier, Amsterdam, 2016.
2. Sundaram, D. S., V. Yang, and E. Zarko, "Combustion of nano aluminum particles (review)," *Comb. Expl. Shock. Waves*, Vol. 51, No. 2, 173–196, 2015.
3. Muthu Gnana Theresa Nathan, D., S. Jacob Melvin Boby, P. Basu, R. Mahesh, S. Harish, S. Joseph, and P. Sagayaraj, "One-pot hydrothermal preparation of Cu_2O-CuO/rGO nanocomposites with enhanced electrochemical performance for supercapacitor applications," *Appl. Surf. Sci.*, Vol. 449, 474–484, 2018.
4. Wilmański, A., M. Bućko, Z. Pędzich, and J. Szczerba, "Salt-assisted SHS synthesis of aluminium nitride powders for refractory applications," *J. Mater. Sci. Chem. Eng.*, Vol. 2, No. 10, 26–31, 2014.
5. Jeong, T., K. H. Kim, S. J. Lee, S. H. Lee, S. R. Jeon, S. H. Lim, J. H. Baek, and J. K. Lee, "Aluminum nitride ceramic substrates-bonded vertical light-emitting diodes," *IEEE Photon. Technol. Lett.*, Vol. 21, No. S3, 890–892, 2009.
6. Hunt, W. H., "New directions in aluminum-based P/M materials for automotive applications," *Int. J. Powd. Metal.*, Vol. 36, No. 6, 50–56, 2000.
7. Ilyin, A. P., L. O. Root, and A. V. Mostovshchikov, "Application of aluminum nanopowder for pure hydrogen production," *Key Eng. Mater.*, Vol. 712, 261–266, 2016.
8. Tan, W. S., V. Bousquet, M. Kauer, K. Takahashi, and J. Heffernan, "InGaN-based blue-violet laser diodes using AlN as the electrical insulator," *Jpn. J. Appl. Phys.*, Vol. 48, No. 7R, 072102, 2009.
9. Aruna, S. T. and A. S. Mukasyan, "Combustion synthesis and nanomaterials," *Curr. Opin. Solid State Mater. Sci.*, Vol. 12, 44–50, 2008.
10. Li, L., A. P. Ilyin, F. A. Gubarev, A. V. Mostovshchikov, and M. S. Klenovskii, "Study of self-propagating high-temperature synthesis of aluminium nitride using a laser monitor," *Ceram. Int.*, Vol. 44, No. 16, 9800–19808, 2018.
11. Gubarev, F. A., M. S. Klenovskii, L. Li, A. V. Mostovshchikov, and A. P. Ilyin, "High-speed visualization of nanopowder combustion in air," *Opt. Pura Apl.*, Vol. 51, No. 4, 51003:1–7, 2018.
12. Gubarev, F. A., A. V. Mostovshchikov, M. S. Klenovskii, A. P. Il'in, and L. Li, "Copper bromide laser monitor for combustion processes visualization," *Progress In Electromagnetic Research Symposium (PIERS)*, *2016 Progress In Electromagnetic Research Symposium (PIERS)*, 2666–2670, Shanghai, China, August 8–11, 2016.
13. McNesby, K. L., B. E. Homan, R. A. Benjamin, V. M. Boyle, J. M. Densmore, and M. M. Biss, "Invited article: Quantitative imaging of explosions with high-speed cameras," *Rev. Sci. Instrum.*, Vol. 87, No. 5, 051301, 2016.
14. Abdel-Hafez, A. A., M. W. Brodt, J. R. Carney, and J. M. Lightstone, "Laser dispersion and ignition of metal fuel particles," *Rev. Sci. Instrum.*, Vol. 82, No. 6, 064101, 2011.
15. Chen, Y., D. R. Guildenbecher, K. N. G. Hoffmeister, M. A. Cooper, H. L. Stauffacher, M. S. Oliver, and E. B. Washburn, "Study of aluminum particle combustion in solid propellant plumes using digital in-line holography and imaging pyrometry," *Combust. Flame*, Vol. 82, 225–237, 2017.
16. Plantier, K. B., M. L. Pantoya, and A. E. Gash, "Combustion wave speeds of nanocomposite Al/Fe_2O_3: The effects of Fe_2O_3 particle synthesis technique," *Combust. Flame*, Vol. 140, No. 4, 299–309, 2005.
17. Lynch, P., G. Fiore, H. Krier, and N. Glumac, "Gas-phase reaction in nanoaluminum combustion," *Combust. Sci. Technol.*, Vol. 182, No. 7, 842–857, 2010.
18. Little, C. E., *Metal Vapor Lasers: Physics, Engineering and Applications*, John Willey & Sons Ltd., Chichester, 1999.
19. Kazaryan, M. A., V. M. Batenin, V. V. Buchanov, A. M. Boichenko, I. I. Klimovskii, and E. I. Molodykh, *High Brightness Metal Vapor Lasers: Physics and Applications*, CRC Press, 2017.

20. Withford, M. J., D. J. W. Brown, R. P. Mildren, R. J. Carman, G. D. Marshall, and J. A. Piper, "Advances in copper laser technology: Kinetic enhancement," *Prog. Quant. Electron.*, Vol. 28, Nos. 3–4, 165–196, 2004.
21. Biswal, R., G. K. Mishra, P. K. Agrawal, S. V. Nakhe, and S. K. Dixit, "Studies on the spectral purity of copper-hydrogen bromide laser radiations," *Appl. Opt.*, Vol. 52, No. 14, 3269–3278, 2013.
22. Gubarev, F. A., L. Li, M. S. Klenovskii, and D. V. Shiyanov, "Spatial-temporal gain distribution of a CuBr vapor brightness amplifier," *Appl. Phys. B*, Vol. 122, 284, 2016.
23. Nekhoroshev, V. O., V. F. Fedorov, G. S. Evtushenko, and S. N. Torgaev, "Copper bromide vapour laser with a pulse repetition rate up to 700 kHz," *Quantum Electron.*, Vol. 42, No. 10, 877–879, 2012.
24. Gubarev, F. A., V. F. Fedorov, K. V. Fedorov, D. V. Shiyanov, and G. S. Evtushenko, "Copper bromide vapour laser with an output pulse duration of up to 320 ns," *Quantum Electron.*, Vol. 46, No. 1, 57–60, 2016.
25. Astadjov, D. N., K. D. Dimitrov, D. R. Jones, V. K. Kirkov, C. E. Little, N. V. Sabotinov, and N. K. Vuchkov, "Copper bromide laser of 120 W average output power," *IEEE J. Quantum Electron.,* Vol. 33, No. 5, 705–709, 1997.
26. Skripnichenko, A. S., A. N. Soldatov, and N. A. Yudin, "Method of two-pulse frequency regulation of copper-vapor laser parameters," *J. Russ. Las. Res.*, Vol. 16, No. 2, 134–137, 1995.
27. Petrash, G. G., *Optical Systems with Brightness Amplifiers*, Nauka, Moscow, 1991.
28. Buzhinsky, R. O., V. V. Savransky, K. I. Zemskov, A. A. Isaev, and O. I. Buzhinsky, "Observation of objects under intense plasma background illumination," *Plasma Phys. Rep.,* Vol. 36, No. 13, 1269–1271, 2010.
29. Abramov, D. V., S. M. Arakelian, A. F. Galkin, I. I. Klimovskii, A. O. Kucherik, and V. G. Prokoshev, "On the possibility of studying the temporal evolution of a surface relief directly during exposure to high-power radiation," *Quantum Electron.*, Vol. 36, No. 6, 569–575, 2006.
30. Kuznetsov, A. P., R. O. Buzhinskij, K. L. Gubskii, A. S. Savjolov, S. A. Sarantsev, and A. N. Terekhin, "Visualization of plasma-induced processes by a projection system with a Cu-laser-based brightness amplifier," *Plasma Phys. Rep.*, Vol. 36, No. 5, 428–437, 2010.
31. Gubarev, F. A., M. S. Klenovskii, and L. Li, "A mirror based scheme laser projection microscope," *IOP Conf. Series: Materials Science and Engineering*, Vol. 81, 012016, 2016.
32. Mironov, E. G., Z. Li, H. T. Hattori, K. Vora, H. H. Tan, and C. Jagadish, "Titanium nano-antenna for high-power pulsed operation," *J. Lightwave Technol.*, Vol. 31, No. 15, 2459–2466, 2013.